The Sustained North American Warming of 1997 and 1998

ARUN KUMAR AND WANQIU WANG

National Centers for Environmental Prediction, Washington, District of Columbia

MARTIN P. HOERLING

National Oceanic and Atmospheric Administration–Cooperative Institute for Research in Environmental Studies, Climate Diagnostics Center, Boulder, Colorado

ANTS LEETMAA AND MING JI

National Centers for Environmental Prediction, Washington, District of Columbia

(Manuscript received 8 November 1999, in final form 24 April 2000)

ABSTRACT

North America experienced sustained and strong surface warming during 1997 and 1998. This period coincided with a dramatic swing of the El Niño–Southern Oscillation (ENSO), with El Niño in 1997 rapidly replaced by La Niña in 1998. An additional aspect of the sea surface temperatures (SSTs) was the warmth of the world oceans as a whole for the entire period, with unprecedented amplitudes within the recent instrumental record. Using a suite of dynamical and empirical model simulations, this study examines the causes for the North American warming, focusing on the role of the sea surface boundary conditions.

Two sets of atmospheric general circulation model experiments, one forced with the observed global SSTs and the other with the tropical east Pacific portion only, produce similar North American–wide warming during fall and winter of 1997. The GCM results match empirical estimates of the canonical temperature response related to a strong El Niño and confirm that east equatorial Pacific SST forcing was a major factor in the continental warming of 1997.

Perpetuation of that warming from spring through fall of 1998 is shown to be unrelated to equatorial east Pacific SSTs and thus cannot be attributed to the ENSO cycle directly. Yet, simulations using the observed global SSTs are shown to reproduce realistically the continuation of North American warming throughout 1998. The continental warmth occurs in tandem with a warming of the troposphere that, initially confined to tropical latitudes during El Niño's peak in 1997, spreads poleward and covers the entire globe in 1998. This evolutionary aspect of the global circulation anomalies during 1997 and 1998 is found to be a response to global SSTs and not linked directly to ENSO's evolution.

Results presented here demonstrate that a significant fraction of the North American warming in 1997 and 1998 is explainable as the forced response to sea surface boundary conditions. The hand-over in the impact of those SSTs, with a classic ENSO driven signal in 1997 but an outwardly independent signal in 1998 related to the disposition of global SSTs outside the ENSO region is emphasized. The high potential predictability of North American climate during this 2-yr period raises new questions on the role of global SSTs in climate variability and the ability to predict them skillfully.

1. Introduction

At the height of El Niño's strength during boreal winter of 1997–98, North American land temperatures were pervasively warm, though in a manner consistent with the known impacts of much above normal equatorial Pacific sea surface temperatures (SSTs) (Ropelewski and Halpert 1986; Kiladis and Diaz 1989). Indeed, key aspects of North American temperature and precipitation during that winter were skillfully predicted (Barnston et al. 1999; Mason et al. 1999). Success of the forecasts, a scientific understanding of the cause for the extreme winter, and society's preparedness for that event speak to the progress from two decades of El Niño–Southern Oscillation (ENSO) research, spurred in many ways by the previous extreme 1982–83 El Niño.

What makes 1997–98 particularly noteworthy is that unprecedented warming of North America continued during the subsequent spring, summer, and fall seasons of 1998, despite the sign reversal in equatorial Pacific SST anomalies as La Niña quickly followed El Niño

Corresponding author address: Dr. Arun Kumar, Climate Modeling Branch, EMC/NCEP, 5200 Auth Road, Room 807, Camp Springs, MD 20746.
E-mail: arun.kumar@noaa.gov

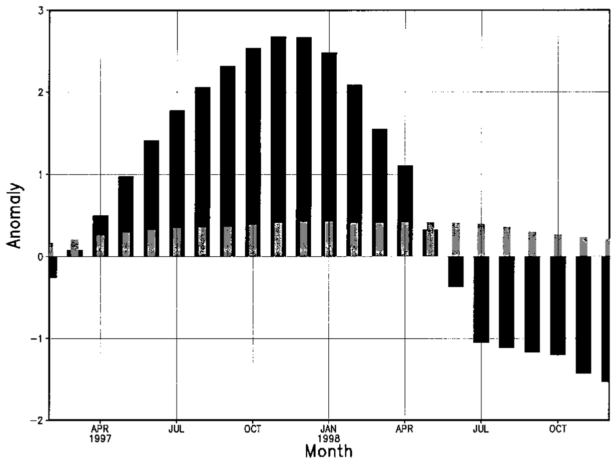

FIG. 1. Temporal evolution of the observed SST anomalies area averaged over the Niño-3.4 index region (black bars). Also shown are the globally averaged SST anomalies for the same period (inserted gray bars). The Niño-3.4 region is defined as the spatial domain extending from 170° to 120°W and 5°S to 5°N. Anomalies are in degrees Celsius and are plotted for successive 3-month seasons.

(Fig. 1). To be sure, a significant fraction of seasonal climate variations in the midlatitudes occurs irrespective of ENSO (e.g., Kumar and Hoerling 1997). Yet, it remains an open question as to whether SST forcings other than ENSO can at times exert important and detectable influences. This question is of particular relevance for the 1997 and 1998 periods because, just as North American temperatures stayed above normal, so too did the global SSTs. Indeed, globally averaged SSTs in 1998 exhibited unprecedented warmth, exceeding by a factor of 2 the warmest global average anomaly of the last half century.

Our purpose in this paper is to seek an attribution for the spring through fall 1998 warm North American surface temperature anomalies on the one hand, and to assess their potential predictability on the other. The inquiry focuses both on the impact of the global ocean and on the seasonal dependency of ENSO's midlatitude impacts. For example, to what extent can the prolonged North American warming be reconciled not only with ENSO forcing, but also with its phase reversal? Was the simultaneous occurrence of global ocean and North American warming merely coincidental, or causal in the sense of an ocean-driven response?

To address these issues, we utilize an ensemble of atmospheric general circulation model (AGCM) experiments that employ a hierarchy of the sea surface boundary conditions from January 1997 to December 1998. One set of runs is forced with monthly evolving globally prescribed SSTs, and a second set is forced only with the tropical east Pacific portion of these SSTs. Also, an empirical model that describes the relation between ENSO and global climate is used as a benchmark against which to compare the simulations from the AGCMs. The models employed, including the experimental details, are described in section 2. The results of our parallel analysis of simulations from dynamical and empirical models are presented in section 3, and a summary is provided in section 4.

2. Observed and model datasets

Observed North American surface temperatures are based on 2.5° latitude/longitude gridded monthly analyses derived from the global network of surface observations maintained at the National Centers for Environmental Prediction (NCEP) (Ropelewski et al. 1985). Atmospheric circulation patterns during this period are based on analysis of global monthly 200-mb height data derived from the NCEP–NCAR reanalysis dataset. Monthly temperature and height anomalies for the January 1997–December 1998 period are calculated relative to their 1950–96 means.

Global sea surface temperatures for 1997–98 are based on the optimum interpolation (OI) analyses of Reynolds and Smith (1994), and are available on a 2° latitude/longitude grid. The historical SST dataset spanning 1950–96 consists of an eigenvector reconstruction for 1950–81 as described in Smith et al. (1996), and the OI analyses for the post-1982 period. Monthly anomalies are again based on a 1950–96 SST climatology.

Interannual SST variability within the Niño-3.4 index region (170°–120°W, 5°N–5°S) is used to construct an empirical model system for North American temperature and global 200-mb height. One-sided linear regressions are performed separately for the warm and the cold phases of the SST index. This approach is used in lieu of the conventional regression analysis because of the known nonlinear relationship between the phase of tropical Pacific SSTs and North American climate (Hoerling et al. 1997, 2001). Our procedure assumes a linear relation between positive and negative signs of the SSTs and a predictand separately, and we calculate such relationships for each calendar month using 1950–96 as a training period.

The empirical model is applied to independent data by scaling the monthly regression maps by the amplitude of the Niño-3.4 SST anomalies for each month from January 1997 to December 1998. The resulting monthly anomalies of North American temperature and 200-mb height represent an empirical estimate of the atmospheric response to the observed Niño-3.4 SST anomalies during that period.

The observed monthly mean SSTs for this 2-yr period are also used to force NCEP's climate model, referred to as MRF9 in previous studies (e.g., Kumar et al. 1996). This is the atmospheric component of the coupled seasonal forecast system at NCEP (Ji et al. 1994), and is a spectral model employing triangular T40 truncation for horizontal discretization, and 18 unequally spaced sigma levels for vertical discretization. Further details of the model appear in Kumar et al. (1996).

For one suite of runs, referred to as Global Ocean–Global Atmosphere (GOGA) simulations, the atmospheric model is forced at the lower boundary with the monthly evolving global SSTs from January 1997 to December 1998. For a second suite of runs, referred to as Pacific Ocean–Global Atmosphere (POGA) simulations, the observed SSTs are specified only over the spatial domain extending from the dateline to the South American coast and from 15°S to 15°N. SSTs in other ocean basins are specified to evolve through their climatological annual cycle. An 18-member ensemble is performed for each suite by repeating the simulations from different model-based atmospheric initial states on 1 January 1997. Simulated surface temperature and 200-mb height anomalies are calculated with respect to the GCM's 1950–96 climatology that is obtained from an existing suite of simulations described in Kumar and Hoerling (1997).

3. Results

Niño-3.4 sea surface temperatures became warmer than normal in spring 1997, followed by a rapid ramp to peak warm anomalies in fall 1997 (Fig. 1). The subsequent decline in SSTs was no less spectacular, with the emergence of below normal values in the Niño 3.4 region by early spring 1998 and mature La Niña conditions by late summer. In contrast, as shown by the inserted bars of Fig. 1, globally averaged SSTs were above normal throughout the 2-yr period. Indeed, whereas the 1997 El Niño was among the strongest of the last half century (e.g., Wolter and Timlin 1998), the global SSTs achieved unprecedented warmth, exceeding by a factor of 2 the previous largest positive anomaly observed since 1950 (not shown).

Coinciding with the onset of equatorial Pacific warming, surface air temperature averaged over North America (20°–70°N, 180°–60°W) became warmer than normal in summer 1997 and achieved peak anomalies during winter (Fig. 2). Only a modest decline from the peak value occurred during 1998, and in fact the subsequent warmth was more extreme when measured as standardized anomalies.

As a first step toward determining an SST attribution for the prolonged North American warming, we compare observed and simulated seasonal anomalies for the boreal winter [December–February (DJF)] of 1997–98. Results from our suite of model simulations of the atmospheric response near the 1997 El Niño peak are consistent with the wintertime global impact of warm equatorial Pacific SSTs found in previous studies. The ensemble GOGA response (Fig. 3 upper-right panel) includes a wavetrain of alternating high and low pressure centers extending from the tropical Pacific across the Pacific–North American region, in close agreement with the observed circulation anomalies (Fig. 3 upper-left panel). The ensemble POGA response (Fig. 3 lower-left panel) is almost indistinguishable from its GOGA

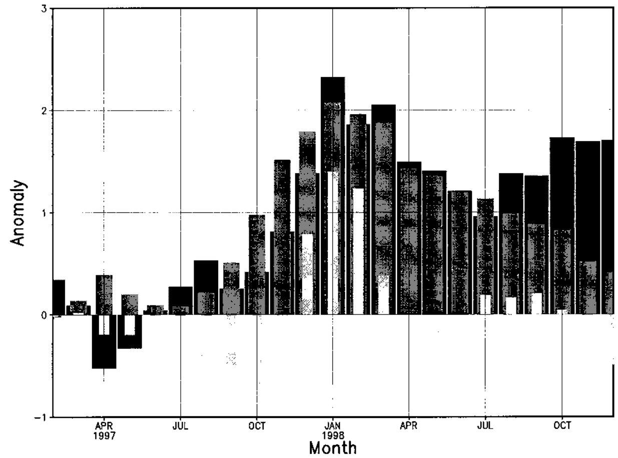

FIG. 2. Surface air temperature anomalies over North America for observations (large bars), GOGA simulations (first inserted bars), and for the empirical model (innermost inserted bars). The domain consists of all the land points between 20° and 70°N and 180° and 60°W. Anomalies are in degrees Celsius and are plotted for successive 3-month seasons.

counterpart indicating that a dominant part of the observed anomalies during the winter season were due to SST anomalies in the east equatorial Pacific alone. This conclusion is further strengthened by the simulated height pattern using the empirical model (Fig. 3 lower-right panel) which, though using only the Niño-3.4 SSTs as a predictor, reproduce much of the climate anomalies of the dynamical models. Taken as a whole, historical statistical effects of El Niño and the GCM modeled ensemble responses all confirm the strong control that the 1997 El Niño had on North American winter climate.

Consistent with the circulation driven response, North American surface air temperature anomalies during that winter were above normal in the dynamical and empirical model simulations. This is illustrated by the inserted bars of Fig. 2 in which the first insert denotes the seasonal averaged GOGA response, and the second insert denotes the corresponding empirical model prediction. The ensemble GOGA surface temperature response during DJF 1997–98 is positive, and furthermore with an amplitude close to that observed. The empirical model result is also above normal, though with somewhat reduced strength. Further aspects of the North American warming, including its spatial pattern and the reproducibility among the GCM individual realizations, will be discussed later.

Global circulation anomalies during spring and summer of 1998 appeared to herald a continuation of the atmospheric response to warm ENSO conditions of the previous winter. This feature becomes evident from the analysis of the evolution of the zonal mean 200-mb height anomalies. The zonal averages of the observed 200-mb height anomalies (Fig. 4, left-side panel) which first became positive in the Tropics one season after initial warming of Niño-3.4 SSTs, exhibited maximum

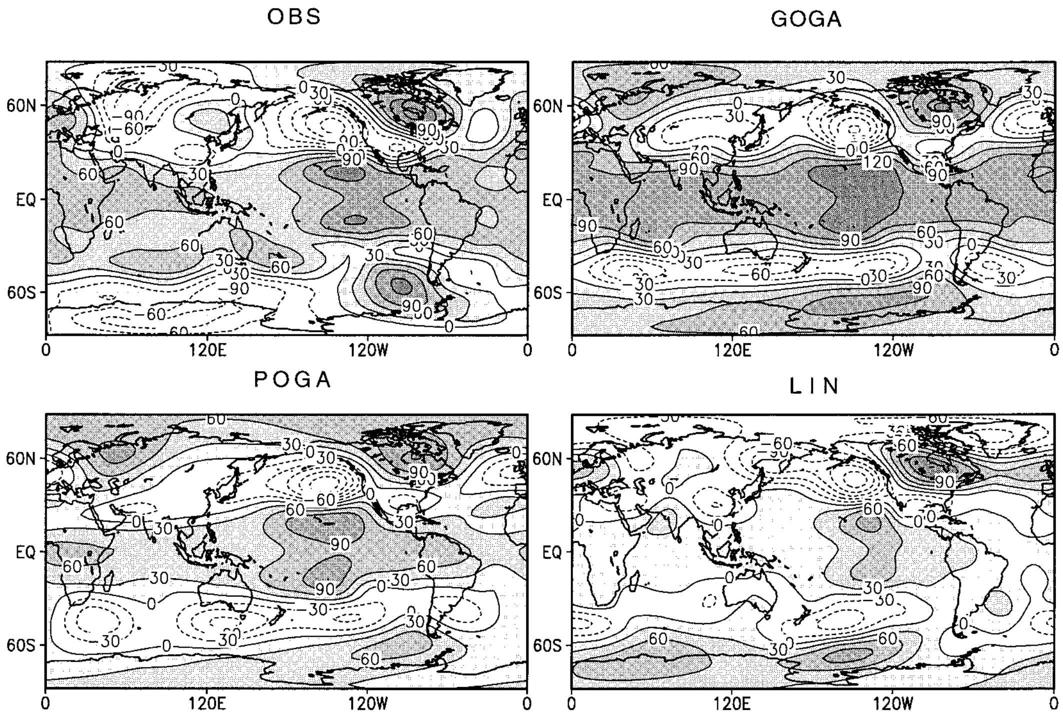

FIG. 3. Dec 1997–Feb 1998 averaged 200-mb height anomalies for observations (upper-left panel), GOGA ensemble simulations (upper-right panel), POGA ensemble simulations (lower-left panel), and for the empirical model (lower-right panel). Regions with positive height anomalies are shaded and dashed contours denote negative anomalies. Contour interval is 30 m.

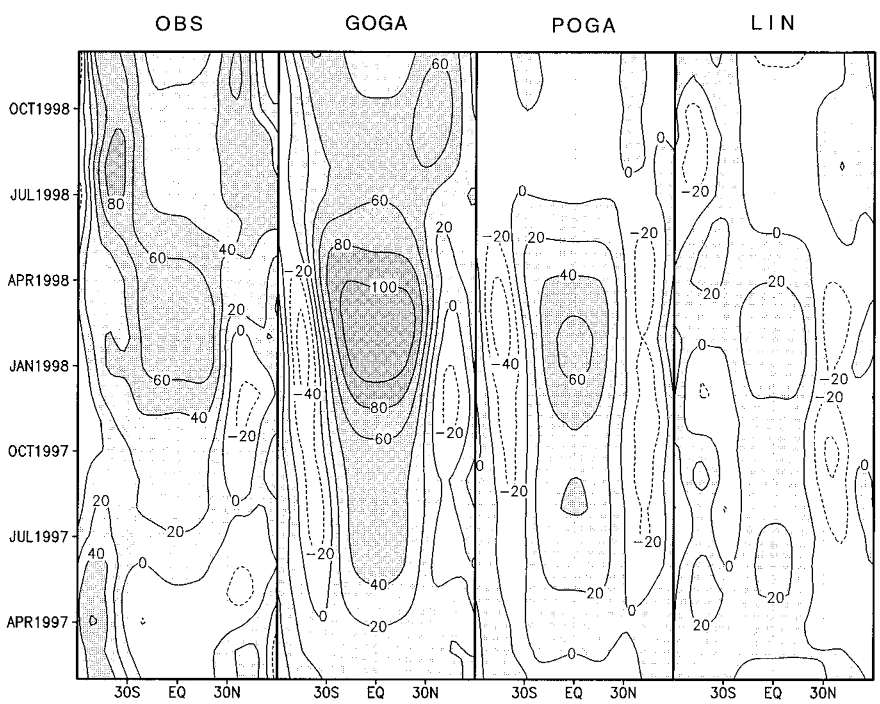

FIG. 4. Time–latitude cross section for zonally averaged 200-mb height anomalies for observations (left panel), GOGA simulations (second from left), POGA simulations (second from right), and empirical model (right panel). Regions with positive height anomalies are shaded. Dashed contours denote negative height anomalies. Contour interval is 20 m. Anomalies are plotted for successive 3-month seasons beginning Feb 1997 (bottom) and ending Nov 1998 (top).

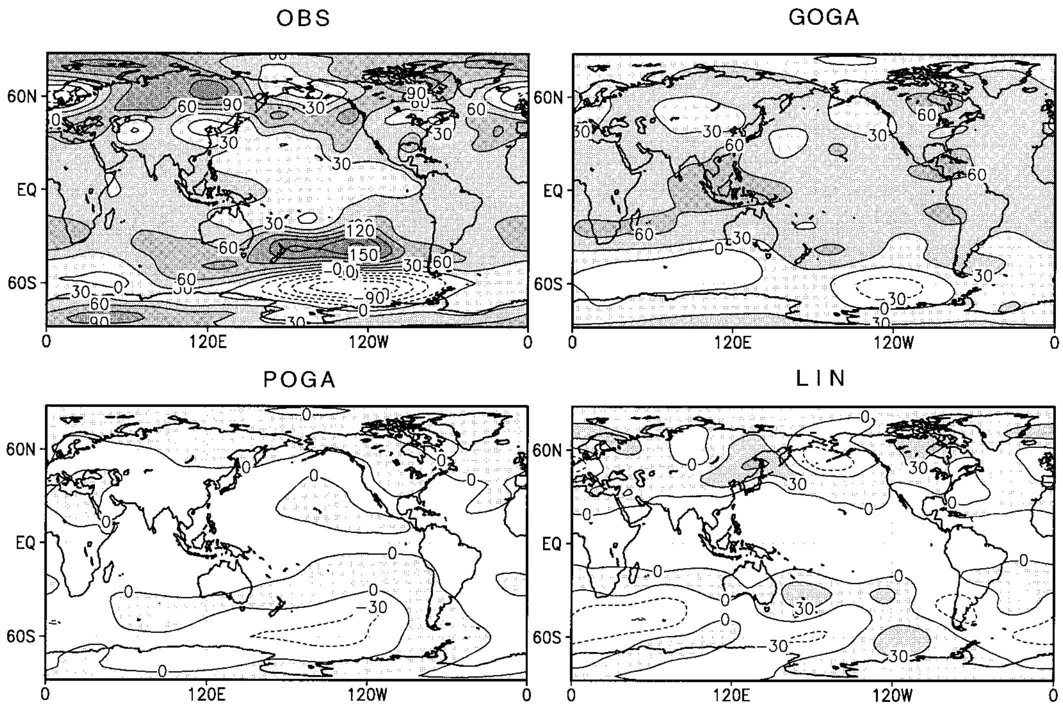

FIG. 5. Same as Fig. 3, but for Jun–Aug 1998 average 200-mb height anomalies.

tropospheric warming well after El Niño's peak. This evolutionary feature has been found in circulation composites related to El Niño (e.g., Angell 1981; Pan and Oort 1983) and appears to be consistent with evidence for a lag in the tropical response to El Niño (e.g., Yulaeva and Wallace 1994).

An additional feature of the time–latitude section is the gradual poleward spreading of above-normal heights into both hemispheres, such that the largest positive height anomalies existed in midlatitudes by summer 1998. The North American surface warming of spring through fall 1998 is intimately related to this upper-level circulation feature. It is unclear, however, to what extent the temporal behavior of the 200-mb anomalies is symptomatic of coherent poleward propagation from tropical sources, or denotes in situ midlatitude development that may be unrelated to antecedent conditions in the equatorial east Pacific.

An intercomparison of the suite of model simulations provides clear evidence for SST forcing of the zonally averaged heights. From spring 1997 until El Niño's peak, the increase in zonal mean tropical heights together with the emergence of below normal midlatitude heights is reproduced in the GOGA, POGA, and empirical model experiments. Though the various simulations differ in amplitude, their similar spatial patterns and agreement with observations for 1997 confirm the importance of tropical east Pacific forcing.

The experiments quickly diverge in spring of 1998, however, and only the GOGA run continues to compare favorably with the observations. Note in particular the simulation of strong midlatitude positive height anomalies in the GOGA runs during the latter half of 1998. The verisimilitude of the GOGA simulations implies that the observed poleward expansion of the original tropically confined warming is consistent with a response to global SSTs. Furthermore, failure to replicate such behavior in either the POGA or empirical models indicates that tropical east Pacific SSTs were not a factor.

To illustrate further the impact of global SSTs, Fig. 5 presents the spatial structure of the observed and modeled 200-mb height anomalies for boreal summer of 1998. Remarkable in the observations is the near-global coverage of above-normal heights, and many of the regional features in nature are also present in the GOGA simulations. By comparison, the POGA and empirical model results compare poorly with observations. In particular the tropical heights are below normal, consistent with the colder SST anomalies in the Niño-3.4 region, but opposite to the observed height anomalies.

It is interesting to note in Fig. 5 that North American 200-mb heights, though weak, are above normal in both the POGA and the empirical models, reflecting the atmospheric response to the La Niña conditions during boreal summer. These results together with the GOGA simulations indicate that atmospheric signals related to both La Niña and the SSTs in the remaining global ocean yielded an in-phase warm thermal response in the extratropics. The separate, though accretive, effects of these boundary forcings can also be seen in the time-longitude diagrams of Fig. 4, where the extratropical

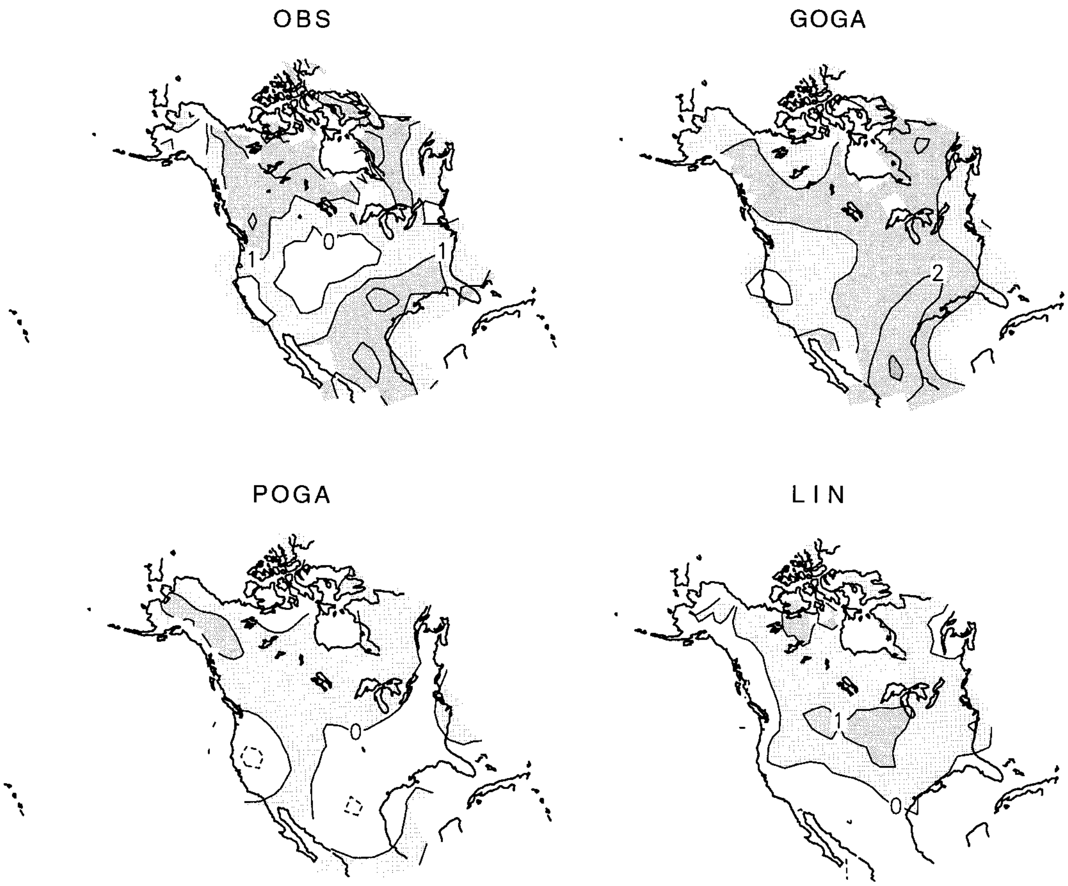

FIG. 6. Jun–Aug 1998 surface air temperature anomalies for observations (upper-left panel), GOGA ensemble simulations (upper-right panel), POGA ensemble simulations (lower-left panel), and empirical model (lower-right panel). Regions with warm temperature anomalies are shaded and dashed contours denote below normal temperature anomalies. Contour interval is 1°C.

zonal mean heights trend toward increasingly positive values during 1998.

Notwithstanding the summertime La Niña signal, the majority of the North American summertime surface warming emerges from non-ENSO reaches of the global oceans. This is evident from the histograms of area, averaged land temperatures in Fig. 2, and also from the spatial distributions of June–August 1998 temperature anomalies shown in Fig. 6. In particular, the observed warming over the southern United States and Mexico are only recreated in the GOGA simulations, whereas these regions experience near or below normal temperatures in response to east equatorial Pacific cold SST forcing alone.

We quantify the level of agreement between observations and the various model results by presenting in Fig. 7 the spatial anomaly correlation over the PNA region (20°–70°N, 180°–60°W) of the seasonally averaged 200-mb heights. For the GOGA simulations (dark, solid line) correlation skill is at or above 0.5 from summer 1997–fall 1998. Note the unanimity in spatial agreement between nature and all simulations in winter 1997, consistent with the strong, and highly predictable, impact of this El Niño on wintertime North American climate anomalies. Importantly, the GOGA experiments retain a high correlation in subsequent seasons, whereas both POGA and empirical model responses experience a sharp decline in skill by spring 1998. Similar correlation results are found for North American surface temperatures (not shown). In particular, only the GOGA experiments maintain a consistently high level of agreement with observed North American temperatures from mid-1997 through 1998.

Whereas the ensemble-averaged GOGA results imply appreciable potential predictability, one cannot discount the possibility that the association with observations for this period is coincidental. It was pointed our earlier that extratropical seasonal mean atmospheric states are not uniquely determined by SST forcing, and in fact the majority of the atmospheric variability is unrelated to SST variability. It is therefore useful to determine the composition of the GCM's ensemble distribution, and evaluate whether the observations resided within the spread of model outcomes for 1997 and 1998. Figure

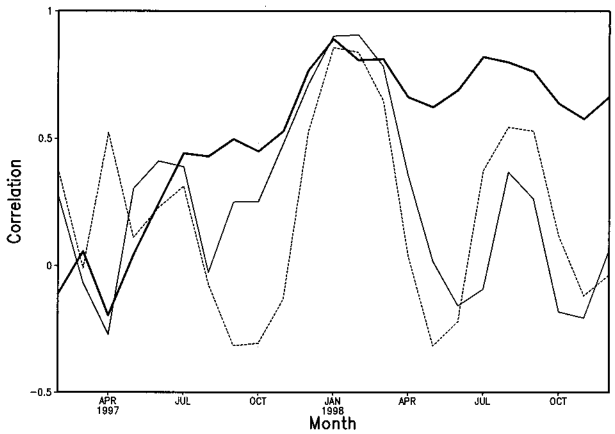

FIG. 7. Spatial correlation between the observed 200-mb height anomalies and GOGA simulations (dark curve), POGA simulations (light curve), and empirical model simulation (dashed curve). The spatial correlation is calculated over the PNA region (180°–60°W and 20°–70°N). The spatial correlations are for successive 3-month seasons.

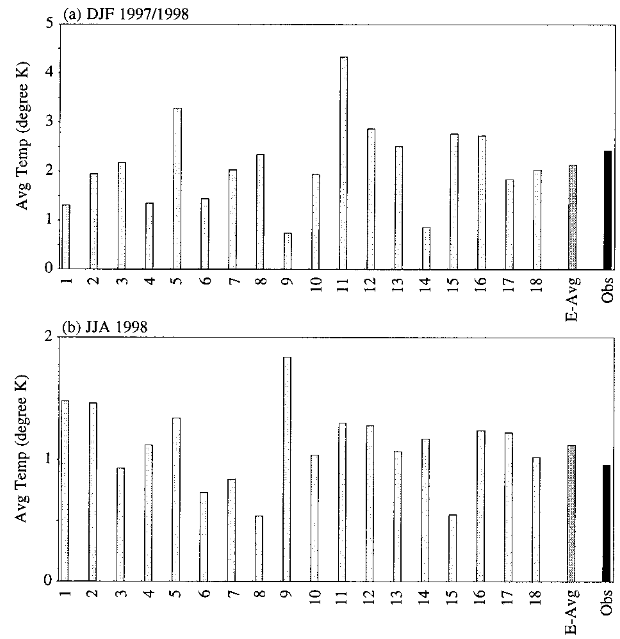

FIG. 8. Surface air temperature anomalies area averaged over North America for each of the 18 member GOGA simulations (light gray bars), ensemble mean GOGA simulation (dark gray bar), and observations (black bar). Top panel is for Dec 1997–Feb 1998, and bottom panel is for Jun–Aug 1998. The domain consists of all the land points between 20° and 70°N and 180° and 60°W. Anomalies are in degrees Celsius.

8 shows the North American area-averaged surface temperature anomalies for winter 1997 (top panel) and summer 1998 (bottom panel) for the individual 18 realizations. For both seasons, each member of the ensemble yields warmer than normal temperatures, though considerable run-to-run variations in amplitude of the warmth is evident. Note that the observations reside well within the ensemble spread. These additional results confirm the reproducibility of prolonged North American warming within the GCM, and indicate the high probability for any single realization for this period, such as is given by the observed data, to have experienced above normal temperatures. The similarity between the GOGA ensemble mean and the observed anomalies would thus appear not to be coincidental, but reflects instead the impact of global SSTs on the probability distribution of seasonal mean atmospheric states.

4. Summary and concluding remarks

This study has sought an attribution for the sustained North American warming that spanned much of 1997 and 1998. Our focus has been on the relationship between this warming and events in the world oceans. Most notable was the extreme ENSO cycle that occurred during the period, with very strong El Niño conditions in 1997 followed by moderate La Niña conditions in 1998. A second, and perhaps related, oceanic event was the warming of the global oceans themselves. This latter warming was embedded within a century-long trend toward higher SSTs, especially in the Tropics (e.g., Knutson and Manabe 1998). The recent warmth appears to be a singular occurrence, however, in that SST anomalies averaged across the world oceans in 1997 and 1998 were twofold greater than in any prior period since 1950.

The results from a suite of dynamical and empirical model simulations for 1997 and 1998 provide evidence for the origin of, and attribution for, the prolonged North American warming. During late 1997 and early 1998, tropical east Pacific SSTs exerted a primary controlling effect. This was confirmed by realistic simulations of the observed extratropical circulation and North American temperature patterns in GCMs using either global SSTs or tropical east Pacific SSTs alone, and also by the results of an empirical model having as its sole predictor Niño-3.4 SSTs. Several recent studies have also demonstrated an ability to account for the late 1997–early 1998 North American climate anomalies as the response to El Niño (e.g., Shukla 1999; Smith et al. 1999). In many ways, the observed continental temperatures were consistent with the canonical signal related to strong El Niño conditions. Furthermore, our analysis of the individual 18-member GCM ensemble revealed a positive North American temperature anomaly in each realization. Indicated here is that the winter seasonal mean signal during El Niño's peak was sufficiently large to ensure a near-deterministic outcome with regard to the sign of the continental temperature anomaly.

It was the perpetuation of the North American warmth through 1998 that was perhaps most interesting and, at first glance, surprising given that tropical east Pacific SSTs reversed sign in April 1998. The warmth during this prolonged period, with little change in its spatial features, led to the impression of influence by a fixed steady forcing. Yet, if a single forcing were indeed responsible, then one needed to reconcile it with the march of the seasonal cycle. Concerning the possible role of east tropical Pacific SSTs, one was confronted with the additional matter of reconciling the reversal in sign of the forcing with the temporal continuity of the hypothesized remote response.

Our suite of model experiments demonstrated a handover in the cause for the North American warming from 1997 to 1998. The rapid weakening of tropical east Pacific SST anomalies in late winter led to a commensurate weakening of the midlatitude impacts. However, a strong signal associated with the state of global SSTs existed as identified from our comparison of GOGA and POGA ensemble simulations. The global SSTs exerted the principal control on North American climate during spring through autumn of 1998, with the GOGA simulations reproducing the sign and spatial pattern of North American temperatures. As in the previous winter, each GOGA realization for the summer of 1998 yielded above normal North American temperatures indicative of a strong SST forced signal.

This signal originated from a pervasively warm troposphere, which by spring of 1998 blanketed virtually the entire globe. The GOGA 200-mb height simulations, mimicking the observed 200-mb height evolution during the 2-yr period, captured the poleward spreading of positive height anomalies from the Tropics in 1997 to middle and high latitudes of both hemispheres in 1998. Such behavior could not be modeled as a response to tropical east Pacific SSTs only. It is worth mentioning, however, that both the POGA and the empirical model simulations indicated a weak North American warming during summer 1998 associated with a La Niña signal, though this was an order of magnitude weaker than the GOGA signal and the actual observed anomaly.

Our results indicate that the sustained North American warming of 1997–98 can be understood as the atmospheric response to global sea surface boundary conditions, and as such the warming is judged to be potentially predictable. During 1998, that response had little to do with boundary forcings in the ENSO region. Rather, the GOGA simulations indicate a large predictable signal related to SSTs in the remainder of the global ocean. Our experiments are unable to explain what aspect of the global oceans were responsible for this signal, however. It has been our initial hypothesis that the warmth of the world oceans as a whole was the important element. This supposition is based on the fact that the simulated 200-mb height anomalies in 1998 were everywhere above normal. Indeed, the spring through autumn 1998 height anomaly patterns are quite featureless and uniform, and it is difficult to identify a local source for the response. This is to be contrasted with winter 1997 when a well-defined wavetrain pattern can be linked to a local tropical Pacific source region, consistent with theoretical expectations (e.g., Hoskins and Karoly 1981; Simmons 1982). It is unclear to what degree the response in 1998 is sensitive to the spatial details of the global SST anomalies, and it also unclear what the relative roles of tropical versus extratropical SST anomalies were.

A related question is the predictability of global SSTs outside of the ENSO region. Current forecast capabilities for skillful SST predictions do not extend appreciably beyond the tropical Pacific. However, aspects of interannual SST variability in other ocean basins have been shown to be related to ENSO via atmospheric bridging mechanisms (e.g., Alexander 1990; Lau and Nath 1996; Klein et al. 1999). For 1997–98 in particular, Yu and Rienecker (1999) found that the observed Indian Ocean SST anomalies could have been induced by the changes in the atmospheric circulation attributable to the El Niño. These results imply that, in addition to the predictability of the east equatorial Pacific SSTs, other aspects of the global SSTs may have been predictable during 1997–98. It will be important to ascertain which SSTs outside the tropical east Pacific were important for the North American warming signal. The extent to which those can be identified and predicted will ultimately determine whether the North American warming that protracted across 1998 was itself predictable.

Acknowledgments. The support offered by NOAA's Climate Dynamics and Experimental Prediction (CDEP) Program is gratefully acknowledged.

REFERENCES

Alexander, M. A., 1990: Simulation of the response of the North Pacific Ocean to the anomalous atmospheric circulation associated with El Niño. *Climate Dyn.,* **5,** 53–65.

Angell, J. K., 1981: Comparisons of variation in atmospheric quantities with sea surface temperature variations in the equatorial eastern Pacific. *Mon. Wea. Rev.,* **109,** 230–242.

Barnston, A. G., and Coauthors, 1999: NCEP forecasts of the El Niño of 1997–98 and its U.S. impacts. *Bull. Amer. Meteor. Soc.,* **80,** 1829–1852.

Hoerling, M. P., A. Kumar, and M. Zhong, 1997: El Niño, La Niña, and the nonlinearity of their teleconnections. *J. Climate,* **10,** 1769–1786.

——, ——, and T.-Y. Xu, 2001: Robustness of the nonlinear climate response to ENSO's extreme phases. *J. Climate,* in press.

Hoskins, B. J., and D. J. Karoly, 1981: The steady state linear response of a spherical atmosphere to thermal and orographic forcing. *J. Atmos. Sci.,* **38,** 1179–1196.

Ji, M., A. Kumar, and A. Leetmaa, 1994: An experimental coupled forecast system at National Meteorological Center: Some early results. *Tellus* **46A,** 398–418.

Kiladis, G. N., and H. F. Diaz, 1989: Global climate anomalies associated with extremes in Southern Oscillation. *J. Climate,* **2,** 1069–1090.

Klein, S. A., B. J. Soden, and N.-C. Lau, 1999: Remote sea surface temperature variations during ENSO: Evidence for a tropical atmosphere bridge. *J. Climate,* **12,** 917–932.

Knutson, T. R., and S. Manabe, 1998: Model assessment of decadal variability and trends in the tropical Pacific Ocean. *J. Climate,* **11,** 2273–2296.

Kumar, A., and M. P. Hoerling, 1997: Interpretation and implications of the observed inter-El Niño variability. *J. Climate,* **10,** 83–91.

——, ——, M. Ji, A. Leetmaa, and P. D. Sardeshmukh, 1996: Assessing a GCM's suitability for making seasonal predictions. *J. Climate,* **9,** 115–129.

Lau, N. C., and M. J. Nath, 1996: The role of atmospheric bridge in linking tropical Pacific ENSO events to extratropical SST anomalies. *J. Climate,* **9,** 2036–2057.

Mason, S. J., and Coauthors, 1999: The IRI seasonal climate prediction system and the 1997/98 El Niño event. *Bull. Amer. Meteor. Soc.,* **80,** 1853–1873.

Pan, Y. H., and A. H. Oort, 1983: Global climate variations connected with sea surface temperature anomalies in the eastern equatorial Pacific Ocean for the 1958–73 period. *Mon. Wea. Rev.,* **111,** 1244–1258.

Reynolds, R. W., and T. M. Smith, 1994: Improved global sea surface temperature analysis using optimum interpolation. *J. Climate,* **7,** 929–948.

Ropelewski, C. F., and M. S. Halpert, 1986: North American precipitation and temperature associated with El Niño–Southern Oscillation (ENSO). *Mon. Wea. Rev.,* **114,** 2352–2362.

——, J. E. Janowiak, and M. S. Halpert, 1985: The analysis and display of real time surface climate data. *Mon. Wea. Rev.,* **113,** 1101–1106.

Shukla, J., 1999: Predictability in the midst of chaos: A scientific basis for climate forecasting. *Science,* **282,** 728–731.

Simmons, A. J., 1982: The forcing of stationary wave motion by tropical diabatic heating. *Quart. J. Roy. Meteor. Soc.,* **108,** 503–534.

Smith, S. R., D. M. Legler, M. J. Remigio, and J. J. O'Brien, 1999: Comparison of 1997–98 U.S. temperature and precipitation anomalies to historical ENSO warm phases. *J. Climate,* **12,** 3507–3515.

Smith, T. M., R. W. Reynolds, R. E. Livezey, and D. Stokes, 1996: Reconstruction of historical sea surface temperatures using empirical orthogonal functions. *J. Climate,* **9,** 1403–1420.

Wolter, K., and M. S. Timlin, 1998: Measuring the strength of ENSO events—How does 1997/98 rank? *Weather,* **53,** 315–324.

Yu, L., and M. M. Rienecker, 1999: Mechanisms for the Indian Ocean warming during 1997–98 El Niño. *Geophys. Res. Lett.,* **26,** 735–738.

Yulaeva, E., and J. M. Wallace, 1994: The signature of ENSO in global temperature and precipitation fields derived from the Microwave Sounding Unit. *J. Climate,* **7,** 1719–1736.